

## Variable Selection in Functional Linear Cox Model

Yuanzhen Yue<sup>1</sup>, Stella Self<sup>1</sup>, Yichao Wu<sup>2</sup>, Jiajia Zhang<sup>1</sup>, and Rahul Ghosal<sup>1,\*</sup>

<sup>1</sup>Department of Epidemiology and Biostatistics, University of South Carolina.

<sup>2</sup>Department of Mathematics, Statistics, and Computer Science, University of Illinois at Chicago.

\**email*: rghosal@mailbox.sc.edu

**SUMMARY:** Modern biomedical studies frequently collect complex, high-dimensional physiological signals using wearables and sensors along with time-to-event outcomes, making efficient variable selection methods crucial for interpretation and improving the accuracy of survival models. We propose a novel variable selection method for a functional linear Cox model with multiple functional and scalar covariates measured at baseline. We utilize a spline-based semiparametric estimation approach for the functional coefficients and a group minimax concave type penalty (MCP), which effectively integrates smoothness and sparsity into the estimation of functional coefficients. An efficient group descent algorithm is used for optimization, and an automated procedure is provided to select optimal values of the smoothing and sparsity parameters. Through simulation studies, we demonstrate the method's ability to perform accurate variable selection and estimation. The method is applied to 2003-06 cohort of the National Health and Nutrition Examination Survey (NHANES) data, identifying the key temporally varying distributional patterns of physical activity and demographic predictors related to all-cause mortality. Our analysis sheds light on the intricate association between daily distributional patterns of physical activity and all-cause mortality among older US adults.

**KEY WORDS:** Functional Cox Model; Variable Selection; NHANES; All Cause Mortality; Physical Activity

This paper has been submitted for consideration for publication in *Biometrics*

## 1. Introduction

Functional data analysis (FDA) ([Ramsay and Silverman, 2005](#); [Crainiceanu et al., 2024](#)) is a statistical framework used to analyze data that can be represented as functions, curves, or trajectories over a continuum such as time, space, or other domains. Unlike traditional multivariate analysis, which focuses on finite-dimensional vectors, FDA deals with infinite-dimensional objects, making it particularly suitable for complex datasets where observations are best understood as smooth curves or surfaces. The applications of FDA are vast and span numerous scientific fields. In the biomedical sciences, FDA is utilized to analyze growth curves ([Ramsay and Silverman, 2007](#)), heart rate ([Ratcliffe et al., 2002](#); [Diller et al., 2006](#)), physical activity ([Xiao et al., 2015](#); [Goldsmith et al., 2016](#); [Cui et al., 2021, 2022](#); [Ghosal et al., 2023](#)), and brain activity patterns ([Tian, 2010](#)) over time, offering deeper insights into physiological processes and health outcomes. Environmental studies benefit from FDA through the analysis of temporal and spatial data, such as climate patterns and pollution levels, allowing for the modeling and prediction of environmental phenomena ([Besse et al., 2000](#)). In finance, FDA is used to model and forecast economic indicators, stock prices, and interest rates, where the continuous nature of the data provides a richer understanding of market behaviors ([Horváth and Kokoszka, 2012](#)).

The integration of FDA and survival analysis is particularly valuable in biomedical research, where continuous monitoring of physiological signals is common. The functional measurements capture detailed temporal variations that may hold important prognostic value for survival outcomes, such as time to disease progression, recurrence, or death. By leveraging FDA, we can effectively model and analyze these functional covariates, enabling a more comprehensive understanding of their relationships with survival outcomes. Functional Cox models ([Gellar et al., 2015](#); [Cui et al., 2021](#)) extend the traditional Cox proportional hazards model ([Cox, 1972](#)) by incorporating functional covariates as predictors. Several

approaches have been proposed for estimation and inference in the functional Cox model (Kong et al., 2018; Hao et al., 2021) and its extensions.

With advancements in technology, the complexity of biomedical data has increased dramatically, especially in modern studies involving high-dimensional physiological signals and time-to-event outcomes. These studies now routinely collect vast amounts of data, posing significant challenges in identifying the high-dimensional variables truly associated with the outcome of interest. Robust variable selection methods are therefore crucial for improving interpretation and accuracy of such high-dimensional models (Hastie et al., 2015). Several methods have been developed for variable selection in “classical” survival models with scalar covariates based on penalized likelihood approaches such as least absolute shrinkage and selection operator (LASSO) (Tibshirani, 1997; Simon et al., 2011), elastic net (Wu, 2012), and other nonconcave extensions (Fan and Li, 2002; Du et al., 2010; Honda and Härdle, 2014). In scalar-on-function regression (Reiss et al., 2017; Crainiceanu et al., 2024), several methods have been proposed to perform variable selection that select the relevant functional predictors (Gertheiss et al., 2013; Ma, 2016; Collazos et al., 2016), as well as estimate their smooth dynamic association with the scalar outcome of interest.

Despite the increasing collection of high-dimensional functional observations, such as physical activity, heart rate, and energy expenditure, existing literature on variable selection in survival models that address the simultaneous selection of functional and scalar covariates is relatively sparse. In our motivating application, we specifically focus on accelerometer data from the 2003-06 waves of the National Health and Nutrition Examination Survey (NHANES). This dataset is linked with the National Death Index (NDI) up to December 31, 2019 (Leroux et al., 2019) to define our survival outcome of interest. Numerous studies in the past in NHANES have demonstrated a consistent link between higher levels of physical activity (PA) and reduced mortality risk (Koster et al., 2012; Saint-Maurice et al., 2020).

Traditionally, these models have been based on summary-level PA metrics (Leroux et al., 2019; Smirnova et al., 2020; Ledbetter et al., 2022; Leroux et al., 2024). Recent methods using a functional Cox model and its extensions have investigated associations of the average daily patterns (Xiao et al., 2015) of physical activity with mortality risk (Cui et al., 2021; Ghosal et al., 2023). Figure 1a displays the average diurnal physical activity counts across all participants, accompanied by detailed activity profiles for five randomly chosen individuals, along with their respective survival times and censoring statuses. Recent research in the area of distributional analysis (Ghosal et al., 2023) has highlighted that distributional features beyond the mean, such as variability and other higher order moments of PA varying through the day, can provide meaningful and complementary information that can enhance insights beyond the average diurnal PA pattern (Varma et al., 2021; Ghosal et al., 2022). The daily time-of-day dependent L-moments (Ghosal et al., 2022; Cho et al., 2024) provide a useful framework for characterizing the daily distributional patterns of physical activity. Figure 1b illustrates the average of the first four diurnal L-moments of physical activity profiles across all participants, as well as the first four diurnal L-moments for five randomly selected participants, based on the log-transformed activity counts. The main objective of our study is to identify the influential functional predictors from the diurnal higher order L-moments of PA, as well as the key demographic and lifestyle covariates which are associated with all-cause mortality among older US adults .

[Figure 1 about here.]

In this paper, we develop a method for variable selection in a functional linear Cox model (FLCM) with multiple functional and scalar covariates measured at the baseline. Our main contributions are three-fold. First, we demonstrate that in a functional linear Cox model with multiple functional and scalar covariates, the variable selection problem can be identified as a group selection problem. Second, we utilize a spline-based semiparametric estimation

approach for the functional coefficients and a group minimax concave type penalty (MCP), which jointly enforces smoothness and sparsity into the estimation of functional coefficients, along with the selection of the scalar covariates. Third, we employ an efficient group descent algorithm for optimization and provide an automatic procedure for choosing the tuning parameters based on an extended Bayesian information type criterion (EBIC) (Chen and Chen, 2008).

The rest of this paper is organized as follows. In Section 2, we present our modeling framework and illustrate our variable-selection method. In Section 3, we conduct a simulation study to evaluate the performance of our method and summarize the results. In Section 4, we apply the proposed variable-selection method to the NHANES 2003-06 accelerometer data and present our findings. We conclude in Section 5 with a discussion and deliberate on some potential extensions of our work.

## 2. Methodology

### 2.1 Modeling Framework

We denote by  $T_i$  the survival time for subject  $i$ , and  $C_i$  the corresponding censoring time for  $i = 1, \dots, n$ . The observed survival time is given by  $Y_i = \min(T_i, C_i)$  in the presence of right censoring, and  $\Delta_i = I(T_i \leq C_i)$  is the event indicator. The scalar baseline covariates are denoted as  $\mathbf{Z}_i = (Z_{i1}, Z_{i2}, \dots, Z_{ip})^T$ . We also observe functional covariates,  $Z_{ik}(s) \in \mathcal{L}^2[0, 1]$ , for  $k = 1, 2, \dots, K$ , for each subject at the baseline. We assume they lie in a real separable Hilbert space, taken to be  $\mathcal{L}^2[0, 1]$  in this paper. In developing our method, we assume these functional covariates are observed on a dense and regular grid of points  $S = \{t_1, t_2, \dots, t_m\} \subset [0, 1]$ , matching our motivating application. Although, this can be relaxed and extended to more general scenarios. Denote the data observed for the  $i$ th subject, as  $D_i = \{T_i, C_i, Y_i, \delta_i, \mathbf{Z}_i, Z_{ik}(s)\}$  (for  $i = 1, 2, \dots, n$ ). We assume that the survival time  $T$  is independent of the censoring time  $C$ , conditional on the scalar and functional covariates.

## 2.2 Functional Linear Cox Model

We posit a functional linear cox model (Gellar et al., 2015) given by:

$$\log h_i(t; \boldsymbol{\beta}, \boldsymbol{\beta}(\cdot)) = \log h_0(t) + \mathbf{Z}_i^T \boldsymbol{\beta} + \sum_{k=1}^K \int_0^1 Z_{ik}(s) \beta_k(s) ds, \quad (1)$$

where  $h_i(t; \boldsymbol{\beta}, \boldsymbol{\beta}(\cdot))$  is the hazard at time  $t$  given covariates  $\mathbf{Z}_i$  and  $\{Z_{ik}(s), k = 1, 2, \dots, K\}$ ,  $h_0(t)$  is the baseline hazard function,  $\boldsymbol{\beta} = (\beta_1, \beta_2, \dots, \beta_p)^T$  are scalar parameters associated with log hazard ratio of the scalar covariates. The functional parameters  $\beta_k(s)$  (for  $k = 1, 2, \dots, K$ ) are assumed to be smooth with finite second derivatives, and capture the association with the log hazard at index  $s$ . Specifically, a positive value of  $\beta_k(s)$  indicates that an increase in the corresponding functional covariate at time  $s$  is associated with an increase in the log hazard, assuming all other covariates remain unchanged.

We model the unknown coefficient functions  $\beta_k(s)$  using a set of known basis functions  $\{\theta_{kc}(s), c = 1, 2, \dots, C_k\}$  for  $k = 1, 2, \dots, K$ . The coefficient functions are thus expressed through a basis function expansion as:

$$\beta_k(s) = \sum_{c=1}^{C_k} b_{kc} \theta_{kc}(s) = \boldsymbol{\theta}_k(s)^T \mathbf{b}_k,$$

where  $\boldsymbol{\theta}_k(s) = (\theta_{k1}(s), \theta_{k2}(s), \dots, \theta_{kC_k}(s))^T$ , and  $\mathbf{b}_k = (b_{k1}, b_{k2}, \dots, b_{kC_k})^T$  is a vector of unknown coefficients. Throughout this paper, we employ B-spline basis functions, though other basis functions may also be used.

We use a penalized partial log-likelihood approach (Gellar et al., 2015; Cui et al., 2021) for estimation of the unknown parameters. The partial likelihood (Gellar et al., 2015) for a functional linear Cox model (FLCM) is given by

$$L(\boldsymbol{\beta}, \boldsymbol{\beta}(\cdot)) = \prod_{d \in D} \frac{\exp(\eta_d)}{\sum_{r \in R_d} \exp(\eta_r)}, \quad (2)$$

where  $D$  is the set of failure indices,  $R_d$  is the set of individuals at risk at time  $t_d$ , and  $\eta_i$  is the systematic component of our model defined as:  $\eta_i = \sum_{j=1}^p Z_{ij} \beta_j + \sum_{k=1}^K \int_0^1 Z_{ik}(s) \beta_k(s) ds$ . The log partial likelihood is denoted by:  $\ell(\boldsymbol{\beta}, \boldsymbol{\beta}(\cdot)) = \log L(\boldsymbol{\beta}, \boldsymbol{\beta}(\cdot))$ .

Since, we are interested in smooth estimation of the functional coefficients (Gellar et al., 2015) as well as imposing sparsity (Gertheiss et al., 2013; Ghosal et al., 2020), we impose a penalty on the log partial likelihood to ensure both sparsity and smoothness. We apply separate penalties to the scalar and functional parameters to account for the smoothness of the functional parameters. For scalar parameters, penalties like LASSO (Tibshirani, 1996), MCP (Zhang, 2010), etc., can be applied for performing variable selection. For example, the LASSO penalty is defined as  $P_\lambda\{\beta_j\} = \lambda\|\beta_j\|_1$ , which effectively shrinks certain coefficients to zero, thereby eliminating non-informative predictors from the model. Since the functional coefficients are assumed to be smooth, we impose a penalty on the roughness of the coefficient functions  $\beta_k(s)$  as follows:

$$\begin{aligned} P_{\lambda,\psi}\{\beta_k(\cdot)\} &= \lambda \left\{ \int \beta_k(\cdot)^2 dt + \psi \int \beta_k''(\cdot)^2 dt \right\}^{1/2} \\ &= \lambda (\mathbf{b}_k^T \mathbb{R}_k \mathbf{b}_k + \psi \mathbf{b}_k^T \mathbb{Q}_k \mathbf{b}_k)^{1/2} \\ &= \lambda (\mathbf{b}_k^T \mathbb{K}_{\psi,k} \mathbf{b}_k)^{1/2}, \end{aligned} \quad (3)$$

where  $\mathbb{K}_{\psi,k} = \mathbb{R}_k + \psi \mathbb{Q}_k$ ,  $\mathbb{R}_k = \int \boldsymbol{\theta}_k(s) \boldsymbol{\theta}_k(s)^T dt$ , and  $\mathbb{Q}_k = \int \boldsymbol{\theta}_k''(s) \boldsymbol{\theta}_k''(s)^T dt$ . The parameter  $\psi \geq 0$  determines the degree of penalization for the roughness.

Using the Cholesky decomposition  $\mathbb{K}_{\psi,k} = \mathbb{L}_{\psi,k} \mathbb{L}_{\psi,k}^T$  (Gertheiss et al., 2013; Ghosal et al., 2020) and defining  $\boldsymbol{\gamma}_k = \mathbb{L}_{\psi,k}^T \mathbf{b}_k$ , equation (3) can be reparameterized as:  $P_{\lambda,\psi}\{\beta_k(\cdot)\} = \lambda(\boldsymbol{\gamma}_k^T \boldsymbol{\gamma}_k)^{1/2} = \lambda\|\boldsymbol{\gamma}_k\|_2$ . The systematic component can now be reformulated as,

$$\begin{aligned} \eta_i &= \sum_{j=1}^p Z_{ij} \beta_j + \sum_{k=1}^K \int_0^1 Z_{ik}(s) \beta_k(s) ds \\ &= \sum_{j=1}^p Z_{ij} \beta_j + \sum_{k=1}^K \int_0^1 Z_{ik}(s) \left( \sum_{c=1}^{C_k} b_{kc} \theta_{kc}(s) \right) ds \\ &= \sum_{j=1}^p Z_{ij} \beta_j + \sum_{k=1}^K \sum_{c=1}^{C_k} \left( b_{kc} \cdot \frac{1}{m} \sum_{s=0}^1 Z_{ik}(s) \theta_{kc}(s) \right) \\ &= \sum_{j=1}^p Z_{ij} \beta_j + \sum_{k=1}^K \sum_{c=1}^{C_k} (b_{kc} \cdot Z_{ikc}^*) \end{aligned} \quad (4)$$

$$\begin{aligned}\eta_i &= \sum_{j=1}^p Z_{ij} \beta_j + \sum_{k=1}^K \mathbf{Z}_{ik}^{*T} \cdot \mathbf{b}_k \\ &= \sum_{j=1}^p Z_{ij} \beta_j + \sum_{k=1}^K \tilde{\mathbf{Z}}_{ik}^T \cdot \boldsymbol{\gamma}_k,\end{aligned}$$

where  $m$  is the number of grid points over the interval  $[0, 1]$ ,  $Z_{ikc}^* = \frac{1}{m} \sum_{s=0}^1 Z_{ik}(s) \theta_{kc}(s)$ ,  $\mathbf{Z}_{ik}^* = (Z_{ik1}^*, Z_{ik2}^*, \dots, Z_{ikC_k}^*)^T$ ,  $\tilde{\mathbf{Z}}_{ik} = \mathbf{Z}_{ik}^* \cdot (\mathbb{L}_{\psi, k}^T)^{-1}$  and  $\boldsymbol{\gamma} = (\boldsymbol{\gamma}_1^T, \dots, \boldsymbol{\gamma}_K^T)^T$ .

We recognize the variable selection in our functional linear Cox model can be addressed as a group selection problem, where the grouping is determined by the covariates ( $\tilde{\mathbf{Z}}_{ik}$  (corresponding to each functional predictor)). For example, we can obtain estimates of  $\boldsymbol{\beta}$  and  $\boldsymbol{\gamma}$  by minimizing a penalized log partial likelihood criterion with group LASSO penalty (Yuan and Lin, 2006) on the basis coefficients, and a LASSO penalty on the coefficients of the scalar covariates,

$$\begin{aligned}(\hat{\boldsymbol{\beta}}, \hat{\boldsymbol{\gamma}}) &= \arg \min_{\boldsymbol{\beta}, \boldsymbol{\gamma}} \left\{ \frac{1}{n} (-2\ell(\boldsymbol{\beta}, \boldsymbol{\beta}(\cdot))) + \sum_{j=1}^p \lambda \|\beta_j\|_1 + \sum_{k=1}^K \lambda \|\boldsymbol{\gamma}_k\|_2 \right\} \\ &= \arg \min_{\boldsymbol{\beta}, \boldsymbol{\gamma}} \left\{ \frac{1}{n} (-2\ell(\boldsymbol{\beta}, \boldsymbol{\beta}(\cdot))) + \sum_{j=1}^p P_{\text{LASSO}, \lambda}(\|\beta_j\|_1) + \sum_{k=1}^K P_{\text{LASSO}, \lambda}(\|\boldsymbol{\gamma}_k\|_2) \right\}.\end{aligned}\tag{5}$$

### 2.3 VSFCOX Method for Variable Selection in FLCM

In this paper, we propose the VSFCOX method for performing variable selection in FLCM, by using a group minimax concave penalty (MCP) (Zhang, 2010) extension of the above optimization criterion (5). Although LASSO (Tibshirani, 1996) is a widely used penalization technique for high-dimensional variable selection, it is well known to exhibit a relatively high false positive rate and lead to biased estimates (Mazumder et al., 2011) due to its over-penalization for larger coefficients. The group Minimax Concave Penalty (MCP) (Zhang, 2010) is a non-convex penalty that reduces the estimation bias by gradually relaxing the penalization on coefficients as their magnitude increases (Breheny and Huang, 2015). MCP thus achieves a balance between sparsity and unbiased estimation, making it particularly

attractive for variable selection in functional regression models (Chen et al., 2016; Ghosal et al., 2020; Ghosal and Maity, 2023). Additionally, MCP is known to possess several desirable theoretical properties, such as the oracle property under standard regularity conditions (Zhang, 2010; Breheny and Huang, 2015), This motivates its use in our VSFCOX method involving the coefficients corresponding to both scalar and functional covariates. The penalized estimation problem for the proposed VSFCOX method is formulated as:

$$(\hat{\boldsymbol{\beta}}, \hat{\boldsymbol{\gamma}}) = \underset{\boldsymbol{\beta}, \boldsymbol{\gamma}}{\operatorname{argmin}} \left\{ \frac{1}{n} (-2\ell(\boldsymbol{\beta}, \boldsymbol{\beta}(\cdot))) + \sum_{j=1}^p P_{MCP, \lambda, \phi}(\|\beta_j\|_1) + \sum_{k=1}^K P_{MCP, \lambda, \phi}(\|\boldsymbol{\gamma}_k\|_2) \right\}, \quad (6)$$

where  $P_{MCP, \lambda, \phi}(|\cdot|)$  is defined as :

$$P_{MCP, \lambda, \phi}(|\cdot|) = \begin{cases} \lambda|\cdot| - \frac{|\cdot|^2}{2\phi} & \text{if } |\cdot| \leq \lambda\phi. \\ .5\lambda^2\phi & \text{if } |\cdot| > \lambda\phi. \end{cases}$$

The penalized estimation criterion (6) for the VSFCOX method can be optimized using a group descent algorithm (Breheny and Huang, 2015). The details of this algorithm are presented in Web Appendix A. We have used the `grpreg` package (Breheny and Huang, 2015) in R for performing the above optimization.

#### 2.4 Adaptive Penalized Estimation

We also explore an adaptive version of our proposed penalty function based on adaptive weights for the penalized estimation criterion. Similar to the adaptive LASSO (Zou, 2006), we define an adaptive penalization scheme (Gertheiss et al., 2013) by introducing weights  $w_k$  and  $v_k$  in the penalty function 3. Specifically, the adaptive penalization approach is based on the penalty:  $P_{\lambda, \psi}\{\beta_k(\cdot)\} = \lambda \left\{ w_k \int \beta_k(t)^2 dt + \psi v_k \int \beta_k''(t)^2 dt \right\}^{1/2}$ , where the weights  $w_k$  and  $v_k$  are chosen in a data-adaptive manner (Meier et al., 2009). These weights are designed to reflect subjective beliefs about the true parameter functions and allow for different levels of shrinkage and smoothness for various covariates. We then use a group-MCP generalization

of the adaptive penalty as in the penalized estimation criterion (6). Denoting the initial estimated coefficient functions  $\beta_k(\cdot)$  by  $\beta_k^{\hat{}}(\cdot)$ , (using any fast methods) the adaptive weights can be defined as  $w_k = 1/\|\beta_k^{\hat{}}(\cdot)\|$  and  $v_k = 1/\|\beta_k^{\hat{\prime\prime}}(\cdot)\|$ , where  $\|\beta_k^{\hat{}}(\cdot)\| = \sqrt{\int \beta_k^{\hat{}}(t)^2 dt}$  is the  $\mathcal{L}^2$  norm of  $\beta_k^{\hat{}}(\cdot)$  (and similar for  $\beta_k^{\hat{\prime\prime}}(\cdot)$ ).

### 2.5 Choosing the tuning parameters

Until now, we have assumed that the sparsity parameter  $\lambda$  and the smoothness parameter  $\psi$  in the penalties were known. To determine the optimal tuning parameters  $\psi$  (for smoothness) and  $\lambda$  (for sparsity), we employ an extended Bayesian information type criterion (EBIC) (Chen and Chen, 2008). The proposed EBIC is defined as  $EBIC(\lambda, \psi) = BIC + 2 \log \binom{p}{\nu}$ , where we denote by  $\nu$  the number of selected scalar and functional variables, and  $p$  denotes the total number of scalar and functional variables. In the context of functional data, we have used this approach for calculating  $\nu$  based on the number of selected functional variables rather than the total number of nonzero basis coefficients. The optimal value of  $(\lambda, \psi)$  is then chosen using a two-dimensional grid search, producing the minimum EBIC. For the tuning parameter  $\phi$ , we use the value 3 for the MCP, following the recommendation of the original authors (Zhang, 2010).

## 3. Simulation Study

### 3.1 Simulation Setup

In this section, we assess the effectiveness of our variable selection method, VSFCOX, through a simulation study. We simulate data from the following FLCM,

$$\log h_i(t; \boldsymbol{\beta}, \boldsymbol{\beta}(\cdot)) = \log h_0(t) + \mathbf{Z}_i^T \boldsymbol{\beta} + \sum_{k=1}^{20} \int_0^1 Z_{ik}(s) \beta_k(s) ds,$$

where  $\boldsymbol{\beta} = (\beta_1, \beta_2, \dots, \beta_{15})^T \in \mathbb{R}^{15}$ , and  $\mathbf{Z}_i = (Z_{i1}, Z_{i2}, \dots, Z_{i15})^T \in \mathbb{R}^{15}$ . The regression parameters are specified as  $\beta_1 = 1$ ,  $\beta_2 = 1.5$ , and  $\beta_3 = 2$ , with the remaining parameters

$\beta_j = 0$  for  $j = 4, 5, 6, \dots, 15$ , indicating that the last 12 scalar covariates are not relevant. We denote by  $S = \{m/100 : m = 0, 1, \dots, M = 100\}$  the grid of time points in  $[0, 1]$ , over which the functional curves are observed. The regression functions are given by  $\beta_1(s) = 3 \cos(\pi s)$ ,  $\beta_2(s) = 4.5 \sin(\pi s)$ ,  $\beta_3(s) = 3.5 \cos(2\pi s) - 5.5 \sin(2\pi s)$ ,  $\beta_4(s) = 4 \cos(2\pi s)$ , and  $\beta_5(s) = 2.5 \sin(2\pi s)$ , with the remaining functions  $\beta_k(s) = 0$  for  $k = 6, 7, 8, \dots, 20$ , indicating that the last 15 functional covariates are not relevant. The scalar covariates  $Z_{ij} \stackrel{\text{iid}}{\sim} Z_j$ , where  $Z_j \sim \text{Uniform}(-1, 1)$ . The functional covariates  $\{Z_k(s), k = 1, 2, \dots, 20\}$  are generated as  $Z_{ik}(s) = \sum_{q=1}^{20} \omega_{ikq} \phi_q(s)$ , where  $\phi_q(s)$  are orthogonal basis polynomials and  $\omega_{ikq}$  are mean zero, independently normally distributed scores with variance  $\sigma_q^2 = 4q$ . The baseline hazard follows an exponential distribution with a rate  $\exp(0.5)$ , resulting in  $\log\{h_0(t)\} = \beta_0 = 0.5$ . The censoring times are drawn independently from an exponential distribution with a rate parameter of  $\frac{1}{\mu_c}$ , where the mean censoring time,  $\mu_c = 10$ . We consider three different sample sizes:  $n \in \{200, 400, 800\}$ . For each sample size, we utilize  $n_d = 200$  Monte Carlo (MC) replications to evaluate our method.

### 3.2 Simulation results

Our primary focus is on selecting the relevant scalar covariates  $Z_1, Z_2, Z_3$  and functional covariates  $Z_1(s), Z_2(s), Z_3(s), Z_4(s), Z_5(s)$ . Additionally, we aim to accurately estimate both the scalar effects  $\beta_1, \beta_2, \beta_3$  and the functional parameter curves  $\beta_1(s), \beta_2(s), \beta_3(s), \beta_4(s), \beta_5(s)$ . We use a cubic B-spline basis with 10 basis functions to model the regression functions  $\beta_k(s)$ . We compare the performance of the proposed VSFCOX against an approach using group LASSO penalty (grpregLASSO). The tuning parameters are automatically selected using the proposed EBIC, incorporating both sparsity and smoothness. Table 1 presents the variable selection performance. Specifically, it reports the true positive rate (TPR) and false positive rate (FPR) for scalar, functional, and all variables combined across three sample sizes. Additionally, the table displays the average model size for each scenario. From the

results, it is evident that VSFCOX consistently performs well in terms of selection accuracy, accurately selecting the relevant variables and discarding the irrelevant ones. Both VSFCOX and gprregLASSO demonstrate a high TPR, indicating perfect recovery of true signals. However, only VSFCOX maintains a low FPR, with zero false positives for functional covariates and a negligible FPR for the scalar covariates, highlighting its robustness in eliminating the irrelevant features. Overall, the results underscore the efficacy of VSFCOX in both scalar and functional variable selection, particularly as sample size increases.

[Table 1 about here.]

Beyond selection performance, VSFCOX also demonstrates strong performance in estimation accuracy. It consistently yields minimal bias and mean squared error (MSE) for the scalar parameters (see Web Table 1) and low mean integrated squared error (MISE) for the functional parameters reported in Table 2. The MISE of the functional estimate  $\beta_k(s)$  is defined as:

$$MISE_k = \frac{1}{n_d} \sum_{d=1}^{n_d} \left( \int_0^1 \left( \hat{\beta}_{kd}(s) - \beta_k(s) \right)^2 ds \right),$$

where  $\hat{\beta}_{kd}(s)$  represents the estimate of  $\beta_k(s)$  for the  $d$ -th generated dataset, and  $n_d$  is the total number of datasets. As the sample size increases, VSFCOX's bias and MSE (and MISE for functional coefficients) steadily decrease, demonstrating its efficiency in the estimation of the scalar and functional coefficients.

[Table 2 about here.]

We display the Monte Carlo mean of the estimated functional coefficients  $\hat{\beta}_k(\cdot)$  ( $k = 1, 2, 3, 4, 5$ ), using our proposed method overlaid on true regression curves in Figure 2 for  $n = 400$ . We also display the Monte-Carlo point-wise 95% confidence intervals (CIs). It can be observed that the VSFCOX method closely tracks the true curves, effectively capturing the underlying functional associations. The results for sample sizes  $n = 200$  and  $n = 800$ ,

which demonstrate similar patterns are displayed in Web Figures 1 and 2. With the increased sample size, the estimates show improved accuracy and reduced variability, as reflected by narrower confidence intervals. Overall, these results highlight that VSFCOX not only excels in variable selection but also provides highly accurate estimates of both scalar and functional parameters.

[Figure 2 about here.]

We also explored adaptive penalized estimation, which demonstrates marginal improvements in the selection performance for smaller sample sizes. We refer to Web Tables 2-4 and Web Figure 3 in the supporting information for the detailed results.

#### **4. Real data application: Modelling All-Cause Mortality in NHANES**

##### **2003-2006**

We apply the VSFCOX method to accelerometer data from the NHANES waves 2003-2006, to identify the key temporally varying distributional patterns of physical activity and demographic, lifestyle predictors associated with all-cause mortality. While numerous studies have established a consistent link between higher levels of PA and reduced mortality risk, majority have relied on scalar summary metrics for PA, such as total activity count (TAC) or moderate-to-vigorous PA (MVPA) (Varma et al., 2017; Yerramalla et al., 2021; Ledbetter et al., 2022). Although these summary-metric-based approaches simplify interpretation, they cannot capture the full spectrum of changes in PA intensities over time (Ghosal et al., 2023). Since PA trends can fluctuate throughout the day, preserving these temporal details is crucial for understanding the circadian rhythm of PA (Xiao et al., 2015) and its implications for all-cause mortality (Cui et al., 2021). Recent research (Ghosal et al., 2022) has also demonstrated that distributional metrics beyond mean PA, such as higher-order moments like variability and skewness, offer valuable and complementary insights to those provided by mean PA alone.

The daily time-of-day dependent L-moments (Ghosal et al., 2022, 2023; Cho et al., 2024) provide a useful framework for characterizing the daily distributional patterns of physical activity beyond the average diurnal PA pattern. We are interested in identifying the key daily distributional patterns of PA related to all-cause mortality among older US adults.

The National Health and Nutrition Examination Survey (NHANES) provides comprehensive health and nutrition statistics for the civilian non-institutionalized US population. NHANES 2003-06 includes objectively measured physical activity data collected by hip-worn accelerometers. Participants were asked to wear a physical activity monitor starting on the day of their exam and to keep wearing it all day and night for seven full days (midnight to midnight), removing it on the morning of the ninth day (Leroux et al., 2019). NHANES data is linked to the National Death Index (NDI) for collecting mortality information. Specifically, we use the 2019 mortality data (as of December 31) from the NDI (<https://www.cdc.gov/nchs/data-linkage/mortality-public.htm>) to define our survival outcome.

Our final sample consists of a total of 2,816 adults aged 50–85 years, who had physical activity monitoring data available for at least ten hours per day over a minimum of four days (Cui et al., 2021; Ghosal et al., 2023). Survival time is measured in years from the end of accelerometer wear, with all subjects censored on December 31, 2019, based on mortality information from the NDI 2019 release. Of the 2816 study participants at baseline, 1117 (39.7%) were deceased, while the remaining 1699 participants were considered right-censored. Web Table 5 presents the descriptive statistics of the complete sample and also stratified by deceased or survivor. The average follow-up time for participants was 12.4 years. Web Figure 4 displays the distribution of the observed survival times and the Kaplan-Meier estimate. The scalar covariates included in our analysis were age ( $Z_1$ ), BMI ( $Z_2$ ), gender ( $Z_3$ ), and smoking status (never (reference), former ( $Z_4$ ) and current ( $Z_5$ )).

We calculate daily time-of-day dependent L-moments to serve as our functional exposures, effectively capturing the time-varying distributional patterns in the PA data (Ghosal et al., 2022). L-moments are robust rank-based analogues of traditional moments (Hosking, 1990; Ghosal et al., 2023). The sample L-moments are linear combinations of order statistics (L-statistics), and can be used to compute quantities analogous to the mean, standard deviation, skewness, and kurtosis, termed  $L_1$  moment (which coincides with mean), L-scale ( $L_2$ ), L-skewness ( $L_3$ ), and L-kurtosis ( $L_4$ ), respectively. In particular, the  $r$ -th order population L-moment of a random variable  $X$  is defined as:

$$L_r = r^{-1} \sum_{k=0}^{r-1} (-1)^k \binom{r-1}{k} E(X_{r-k:r}) \quad r = 1, 2, \dots,$$

where  $X_{1:n} \leq X_{2:n} \leq \dots \leq X_{n:n}$  denote the order statistics of a random sample of size  $n$  drawn from the distribution of  $X$ .

For each participant  $i = 1, \dots, n$ , we denote the log-transformed minute-level physical activity counts for individual  $i$  on day  $j$  at time  $s$  as  $X_{ij}(s)$  for  $j = 1, \dots, n_i$ . The observation times are given by  $S = \{m/60 : m \in 0, 1, 2, \dots, 1439\}$  hours. To capture the daily distributional patterns of physical activity data, we extract the first four diurnal L-moments profiles  $L_{ik}(s)$  ( $k = 1, 2, 3, 4$ ) (Ghosal et al., 2022), where  $L_{ir}(s)$  represents the  $r$ -th L-moment of  $\{X_{ij}(s)\}_{j=1}^{n_i}$  for  $s \in (s - \zeta, s + \zeta)$ , with  $\zeta = \frac{5}{60}$  hour (or 5 minutes). The average smoothed L-moments are displayed in Figure 1b along with the profiles for five randomly selected participants. We define  $Z_{ik}(s) = L_{ik}(s)$  for  $k = 1, 2, 3, 4$ . Additionally, to explore the effect modification by age and gender in the effect of the diurnal L-moments, we incorporate the following interaction terms:  $Z_{ik}(s)$  for  $k = 5, 6, 7, 8$  which are the interactions between age and the first four L-moments; and  $Z_{ik}(s)$  for  $k = 9, 10, 11, 12$  representing the interactions between gender and the first four L-moments. We restrict the focus of our analysis to hours  $s \in [6, 22]$ , corresponding to the time range from 6 a.m. to 10 p.m. since most people are inactive during the night (Ghosal and Maity, 2023) and report zero activity in NHNAES

2003-06 outside this period. Finally, we have 5 scalar covariates and 12 functional covariates in our functional linear Cox model given by:

$$\log h_i(t|Z_{i1}, \dots, Z_{i5}, Z_{i1}(\cdot), \dots, Z_{i12}(\cdot)) = \log h_0(t) + \sum_{j=1}^5 Z_{ij}\beta_j + \sum_{k=1}^{12} \int_6^{22} Z_{ik}(s)\beta_k(s) ds.$$

We applied the proposed VSFCOX method to the above FLCM for selection and estimation of the functional and scalar coefficients. For the functional variables, only the first two L-moments were selected, while all others, including interaction terms, were excluded. Figure 3 displays the estimated functional coefficients  $\hat{\beta}_1(\cdot)$ ,  $\hat{\beta}_2(\cdot)$  of the the first and second diurnal L-moments ( $L_1(\cdot)$  and  $L_2(\cdot)$ ) of PA. The first diurnal L-moment represents the average diurnal PA, while the second diurnal L-moment captures the variability of PA throughout the day. For  $\hat{\beta}_1(s)$ , associated with the first diurnal L-moment, a higher daily mean PA during both the morning period (6 a.m. to 1 p.m.) and dusk (approximately 4 p.m. to 7 p.m.) is found to be associated with a reduced hazard of all-cause mortality. This finding highlights the protective effect of a higher average physical activity during these key periods of the day (Leroux et al., 2019; Cui et al., 2021; Leroux et al., 2024). For  $\hat{\beta}_2(s)$ , associated with the second diurnal L-moment, a higher daily variability in PA ( $L_2(\cdot)$ ) between approximately 9 a.m. and 9 p.m. is found to be associated with a reduced hazard of all-cause mortality. These results suggest that not only the average diurnal PA, but also the variability of PA throughout the day could be an important protective factor against the risk of all-cause mortality (Cho et al., 2024) among older adults, possibly leading to a higher reserve of PA.

[Figure 3 about here.]

Web Table 6 displays the selected scalar predictors along with their estimated effects in the form of hazard ratios. The selected scalar variables are age, gender (female), current smoking, and former smoking. Specifically, age (Leroux et al., 2024), current smoking, and former smoking (Jha et al., 2013) are found to be associated with an increased hazard of all-cause mortality. The hazard associated with current smoking exceeded that of former

smoking, underscoring the severe harm of ongoing smoking (Kenfield et al., 2008). Females are found to have a lower hazard of all-cause mortality (Haukkala et al., 2009) in this study than males, after adjusting for all other predictors.

In additional analysis, we introduced 10 functional pseudo-covariates (Wu et al., 2007; Ghosal et al., 2020) to the original data to rigorously assess the performance of the proposed variable selection approach. These functional pseudo-covariates serve as “noise” to test our method’s specificity and its potential for false-positive selection in high-dimensional case. Specifically, we generate  $Z_{ij}(\cdot) \stackrel{iid}{\sim} Z_j(\cdot)$ , where  $Z_j(h)$  ( $j = 13, 14, \dots, 22$ ) are given by  $Z_j(h) = a_j\sqrt{2}\sin(\pi jh/24) + b_j\sqrt{2}\cos(\pi jh/24)$  with  $a_j \sim \mathcal{N}(0, (2)^2)$ ,  $b_j \sim \mathcal{N}(0, (2)^2)$ . In total, we have 27 covariates, where the first 17 are the original covariates, and the remaining 10 are simulated predictors. We then apply the VSFCOX method to observed survival time and censoring indicator  $\{Y_i, \delta_i\}$ , and the covariates  $Z_{i1}, Z_{i2}, Z_{i3}, \dots, Z_{i1}(s), Z_{i2}(s), \dots, Z_{i22}(s)$ . This process is repeated a large number ( $B = 100$ ) times to observe which variables are selected in each iteration. The selection percentages of the variables are reported in Table 3.

[Table 3 about here.]

Variables such as age, gender (female), former Smoker, current Smoker, and functional predictors diurnal  $L_1(\cdot)$  moment and the diurnal  $L_2(\cdot)$  moment were selected 100% of the time, demonstrating their strong influence on all-cause mortality. In contrast, the remaining original variables and pseudo variables had a selection percentage of 0%, suggesting that they were not deemed relevant in the selection process. This result further highlights the effectiveness of the VSFCOX method in identifying the truly influential predictors while eliminating the irrelevant ones.

## 5. Discussion

In this paper, we proposed a variable selection method in the functional linear Cox model with multiple functional and scalar covariates. Our proposed methodology, VSFCOX, integrates penalized spline-based estimation with a group minimax concave type penalty (MCP), enforcing smoothness and sparsity into the estimation of the functional coefficients. An efficient group descent algorithm is employed for the optimization, and an automated selection criterion is provided for the choice of the tuning parameters.

The simulation results highlighted a satisfactory selection and estimation accuracy of VSFCOX, showing nearly perfect selection consistency for both scalar and functional covariates with increasing sample sizes. The application of our method to the NHANES 2003-06 dataset provided valuable epidemiological insights into the association between daily distributional patterns of PA and all-cause mortality among older US adults. VSFCOX identified the first and second diurnal L-moments ( $L_1(\cdot)$  and  $L_2(\cdot)$ ) of PA, in addition to age, gender, and smoking status, as the key drivers of all-cause mortality among older adults. The results indicate that in addition to daily average PA, daily variability in PA is also a significant determinant of all-cause mortality, after adjusting for age, gender, BMI, and smoking status. These results can be helpful for designing time-of-day (Feng et al., 2023) and intensity-specific PA interventions (Cho et al., 2024).

In this article, we have developed VSFCOX specifically for the functional linear Cox Model. An important future direction would be relaxing the assumption of linearity in covariate effects. In many real-world applications, predictor effects may exhibit nonlinear or more complex patterns that linear models cannot adequately capture. The proposed variable selection method could be extended to accommodate additive models (Cui et al., 2021) which would offer greater flexibility by allowing nonlinear additive effects of the functional and scalar predictors. Sparse single-index models (Jiang et al., 2011; Ma, 2016; Ghosal and

(Maity, 2024) would be another interesting direction to explore, going beyond additive models. If the proportional hazards assumption is not suitable, the variable selection method can be extended to more flexible survival models such as the functional time-transformation model (Ghosal et al., 2025).

In this paper, the primary focus has been on variable selection and estimation of the functional effects. A key challenge in high-dimensional models is that standard inferential tools are no longer directly valid following variable selection using regularized techniques. Future research will therefore explore developing uncertainty quantification methods for the estimated functional effects in VSFCOX using post-selection inference approaches (Lee et al., 2016; Taylor and Tibshirani, 2018) and sample-splitting strategies (Wasserman and Roeder, 2009) that can mitigate the dependency between selection and inference stages.

### **Acknowledgement**

This work is supported by the SPARC Graduate Research grant from the Office of the Vice President for Research, University of South Carolina.

### **Data Availability Statement**

The data supporting the findings of this study are publicly available at <https://www.cdc.gov/nchs/nhanes/continuousnhanes/>.

### **References**

- Besse, P. C., Cardot, H., and Stephenson, D. B. (2000). Autoregressive forecasting of some functional climatic variations. *Scandinavian Journal of Statistics* **27**, 673–687.
- Breheny, P. and Huang, J. (2015). Group descent algorithms for nonconvex penalized linear and logistic regression models with grouped predictors. *Statistics and computing* **25**, 173–187.

- Chen, J. and Chen, Z. (2008). Extended bayesian information criteria for model selection with large model spaces. *Biometrika* **95**, 759–771.
- Chen, Y., Goldsmith, J., and Ogden, R. T. (2016). Variable selection in function-on-scalar regression. *Stat* **5**, 88–101.
- Cho, S. E., Saha, E., Matabuena, M., Wei, J., and Ghosal, R. (2024). Exploring the association between daily distributional patterns of physical activity and cardiovascular mortality risk among older adults in nhanes 2003-2006. *Annals of Epidemiology* **99**, 24–31.
- Collazos, J. A., Dias, R., and Zambom, A. Z. (2016). Consistent variable selection for functional regression models. *Journal of Multivariate Analysis* **146**, 63–71.
- Cox, D. R. (1972). Regression models and life-tables. *Journal of the Royal Statistical Society: Series B (Methodological)* **34**, 187–202.
- Crainiceanu, C. M., Goldsmith, J., Leroux, A., and Cui, E. (2024). *Functional data analysis with R*. CRC Press.
- Cui, E., Crainiceanu, C. M., and Leroux, A. (2021). Additive functional cox model. *Journal of Computational and Graphical Statistics* **30**, 780–793.
- Cui, E., Leroux, A., Smirnova, E., and Crainiceanu, C. M. (2022). Fast univariate inference for longitudinal functional models. *Journal of Computational and Graphical Statistics* **31**, 219–230.
- Diller, G.-P., Dimopoulos, K., Okonko, D., Uebing, A., Broberg, C. S., Babu-Narayan, S., Bayne, S., Poole-Wilson, P. A., Sutton, R., Francis, D. P., et al. (2006). Heart rate response during exercise predicts survival in adults with congenital heart disease. *Journal of the American College of Cardiology* **48**, 1250–1256.
- Du, P., Ma, S., and Liang, H. (2010). Penalized variable selection procedure for cox models with semiparametric relative risk. *Annals of statistics* **38**, 2092.

- Fan, J. and Li, R. (2002). Variable selection for cox's proportional hazards model and frailty model. *The Annals of Statistics* **30**, 74–99.
- Feng, H., Yang, L., Liang, Y. Y., Ai, S., Liu, Y., Liu, Y., Jin, X., Lei, B., Wang, J., Zheng, N., et al. (2023). Associations of timing of physical activity with all-cause and cause-specific mortality in a prospective cohort study. *Nature communications* **14**, 930.
- Gellar, J. E., Colantuoni, E., Needham, D. M., and Crainiceanu, C. M. (2015). Cox regression models with functional covariates for survival data. *Statistical modelling* **15**, 256–278.
- Gertheiss, J., Maity, A., and Staicu, A.-M. (2013). Variable selection in generalized functional linear models. *Stat* **2**, 86–101.
- Ghosal, R. and Maity, A. (2023). Variable selection in nonlinear function-on-scalar regression. *Biometrics* **79**, 292–303.
- Ghosal, R. and Maity, A. (2024). Variable selection in function-on-scalar single-index model via the alternating direction method of multipliers. *TEST* **33**, 106–126.
- Ghosal, R., Maity, A., Clark, T., and Longo, S. B. (2020). Variable selection in functional linear concurrent regression. *Journal of the Royal Statistical Society Series C: Applied Statistics* **69**, 565–587.
- Ghosal, R., Matabuena, M., and Ghosh, S. K. (2025). Functional time transformation model with applications to digital health. *Computational Statistics & Data Analysis* page 108131.
- Ghosal, R., Matabuena, M., and Zhang, J. (2023). Functional proportional hazards mixture cure model with applications in cancer mortality in nhanes and post icu recovery. *Statistical Methods in Medical Research* **32**, 2254–2269.
- Ghosal, R., Varma, V. R., Volfson, D., Hillel, I., Urbanek, J., Hausdorff, J. M., Watts, A., and Zipunnikov, V. (2023). Distributional data analysis via quantile functions and its application to modeling digital biomarkers of gait in alzheimer's disease. *Biostatistics*

**24**, 539–561.

- Ghosal, R., Varma, V. R., Volfson, D., Urbanek, J., Hausdorff, J. M., Watts, A., and Zipunnikov, V. (2022). Scalar on time-by-distribution regression and its application for modelling associations between daily-living physical activity and cognitive functions in alzheimer’s disease. *Scientific reports* **12**, 11558.
- Goldsmith, J., Liu, X., Jacobson, J., and Rundle, A. (2016). New insights into activity patterns in children, found using functional data analyses. *Medicine and Science in Sports and Exercise* **48**, 1723.
- Hao, M., Liu, K.-y., Xu, W., and Zhao, X. (2021). Semiparametric inference for the functional cox model. *Journal of the American Statistical Association* **116**, 1319–1329.
- Hastie, T., Tibshirani, R., and Wainwright, M. (2015). Statistical learning with sparsity. *Monographs on statistics and applied probability* **143**, 8.
- Haukkala, A., Konttinen, H., Uutela, A., Kawachi, I., and Laatikainen, T. (2009). Gender differences in the associations between depressive symptoms, cardiovascular diseases, and all-cause mortality. *Annals of epidemiology* **19**, 623–629.
- Honda, T. and Härdle, W. K. (2014). Variable selection in cox regression models with varying coefficients. *Journal of Statistical Planning and Inference* **148**, 67–81.
- Horváth, L. and Kokoszka, P. (2012). *Inference for functional data with applications*, volume 200. Springer Science & Business Media.
- Hosking, J. R. (1990). L-moments: analysis and estimation of distributions using linear combinations of order statistics. *Journal of the Royal Statistical Society Series B: Statistical Methodology* **52**, 105–124.
- Jha, P., Ramasundarahettige, C., Landsman, V., Rostron, B., Thun, M., Anderson, R. N., McAfee, T., and Peto, R. (2013). 21st-century hazards of smoking and benefits of cessation in the united states. *New England Journal of Medicine* **368**, 341–350.

- Jiang, C.-R., Wang, J.-L., et al. (2011). Functional single index models for longitudinal data. *The Annals of Statistics* **39**, 362–388.
- Kenfield, S. A., Stampfer, M. J., Rosner, B. A., and Colditz, G. A. (2008). Smoking and smoking cessation in relation to mortality in women. *Jama* **299**, 2037–2047.
- Kong, D., Ibrahim, J. G., Lee, E., and Zhu, H. (2018). Flcrm: Functional linear cox regression model. *Biometrics* **74**, 109–117.
- Koster, A., Caserotti, P., Patel, K. V., Matthews, C. E., Berrigan, D., Van Domelen, D. R., Brychta, R. J., Chen, K. Y., and Harris, T. B. (2012). Association of sedentary time with mortality independent of moderate to vigorous physical activity. *PloS one* **7**, e37696.
- Ledbetter, M. K., Tabacu, L., Leroux, A., Crainiceanu, C. M., and Smirnova, E. (2022). Cardiovascular mortality risk prediction using objectively measured physical activity phenotypes in nhanes 2003–2006. *Preventive medicine* **164**, 107303.
- Lee, J. D., Sun, D. L., Sun, Y., and Taylor, J. E. (2016). Exact post-selection inference, with application to the lasso. *The Annals of Statistics* .
- Leroux, A., Cui, E., Smirnova, E., Muschelli, J., Schrack, J. A., and Crainiceanu, C. M. (2024). Nhanes 2011-2014: Objective physical activity is the strongest predictor of all-cause mortality. *Medicine and science in sports and exercise* **56**, 1926–1934.
- Leroux, A., Di, J., Smirnova, E., McGuffey, E. J., Cao, Q., Bayatmokhtari, E., Tabacu, L., Zipunnikov, V., Urbanek, J. K., and Crainiceanu, C. (2019). Organizing and analyzing the activity data in nhanes. *Statistics in biosciences* **11**, 262–287.
- Ma, S. (2016). Estimation and inference in functional single-index models. *Annals of the Institute of Statistical Mathematics* **68**, 181–208.
- Mazumder, R., Friedman, J. H., and Hastie, T. (2011). Sparsenet: Coordinate descent with nonconvex penalties. *Journal of the American Statistical Association* **106**, 1125–1138.
- Meier, L., Van de Geer, S., and Bühlmann, P. (2009). High-dimensional additive modeling.

*The Annals of Statistics* .

- Ramsay, J. and Silverman, B. (2005). *Functional Data Analysis*. Springer-Verlag, New York.
- Ramsay, J. and Silverman, B. (2007). *Applied Functional Data Analysis: Methods and Case Studies*. Springer Series in Statistics. Springer New York.
- Ratcliffe, S. J., Heller, G. Z., and Leader, L. R. (2002). Functional data analysis with application to periodically stimulated foetal heart rate data. ii: Functional logistic regression. *Statistics in medicine* **21**, 1115–1127.
- Reiss, P. T., Goldsmith, J., Shang, H. L., and Ogden, R. T. (2017). Methods for scalar-on-function regression. *International Statistical Review* **85**, 228–249.
- Saint-Maurice, P. F., Troiano, R. P., Bassett, D. R., Graubard, B. I., Carlson, S. A., Shiroma, E. J., Fulton, J. E., and Matthews, C. E. (2020). Association of daily step count and step intensity with mortality among us adults. *Jama* **323**, 1151–1160.
- Simon, N., Friedman, J. H., Hastie, T., and Tibshirani, R. (2011). Regularization paths for cox’s proportional hazards model via coordinate descent. *Journal of statistical software* **39**, 1–13.
- Smirnova, E., Leroux, A., Cao, Q., Tabacu, L., Zipunnikov, V., Crainiceanu, C., and Urbanek, J. K. (2020). The predictive performance of objective measures of physical activity derived from accelerometry data for 5-year all-cause mortality in older adults: National health and nutritional examination survey 2003–2006. *The Journals of Gerontology: Series A* **75**, 1779–1785.
- Taylor, J. and Tibshirani, R. (2018). Post-selection inference for-penalized likelihood models. *Canadian Journal of Statistics* **46**, 41–61.
- Tian, T. S. (2010). Functional data analysis in brain imaging studies. *Frontiers in psychology* **1**, 35.
- Tibshirani, R. (1996). Regression shrinkage and selection via the lasso. *Journal of the Royal*

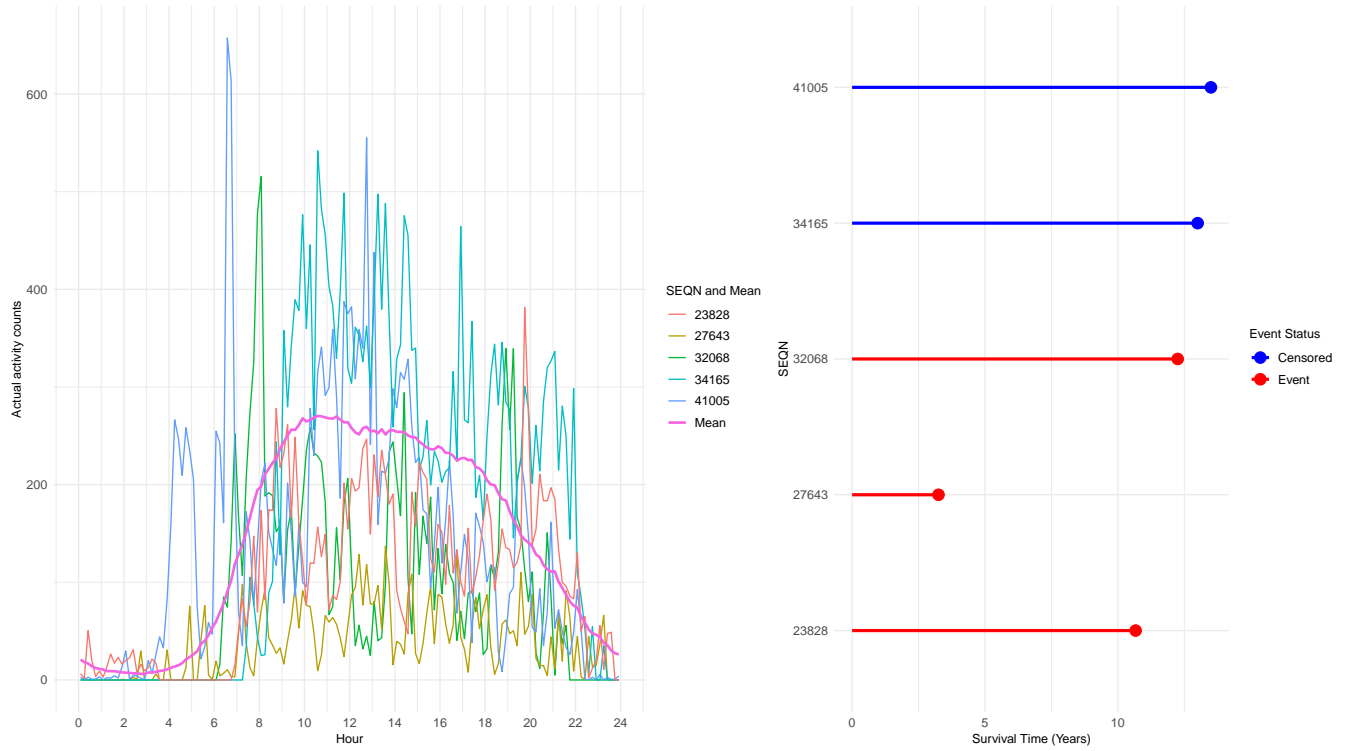
*Statistical Society Series B: Statistical Methodology* **58**, 267–288.

- Tibshirani, R. (1997). The lasso method for variable selection in the cox model. *Statistics in medicine* **16**, 385–395.
- Varma, V. R., Dey, D., Leroux, A., Di, J., Urbanek, J., Xiao, L., and Zipunnikov, V. (2017). Re-evaluating the effect of age on physical activity over the lifespan. *Preventive medicine* **101**, 102–108.
- Varma, V. R., Ghosal, R., Hillel, I., Volfson, D., Weiss, J., Urbanek, J., Hausdorff, J. M., Zipunnikov, V., and Watts, A. (2021). Continuous gait monitoring discriminates community-dwelling mild alzheimer’s disease from cognitively normal controls. *Alzheimer’s & Dementia: Translational Research & Clinical Interventions* **7**, e12131.
- Wasserman, L. and Roeder, K. (2009). High dimensional variable selection. *Annals of statistics* **37**, 2178.
- Wu, Y. (2012). Elastic net for cox’s proportional hazards model with a solution path algorithm. *Statistica Sinica* **22**, 27.
- Wu, Y., Boos, D. D., and Stefanski, L. A. (2007). Controlling variable selection by the addition of pseudovariables. *Journal of the American Statistical Association* **102**, 235–243.
- Xiao, L., Huang, L., Schrack, J. A., Ferrucci, L., Zipunnikov, V., and Crainiceanu, C. M. (2015). Quantifying the lifetime circadian rhythm of physical activity: a covariate-dependent functional approach. *Biostatistics* **16**, 352–367.
- Yerramalla, M. S., McGregor, D. E., van Hees, V. T., Fayosse, A., Dugravot, A., Tabak, A. G., Chen, M., Chastin, S. F., and Sabia, S. (2021). Association of daily composition of physical activity and sedentary behaviour with incidence of cardiovascular disease in older adults. *International Journal of Behavioral Nutrition and Physical Activity* **18**, 1–13.

- Yuan, M. and Lin, Y. (2006). Model selection and estimation in regression with grouped variables. *Journal of the Royal Statistical Society Series B: Statistical Methodology* **68**, 49–67.
- Zhang, C.-H. (2010). Nearly unbiased variable selection under minimax concave penalty. *The Annals of Statistics* **38**, 894–942.
- Zou, H. (2006). The adaptive lasso and its oracle properties. *Journal of the American statistical association* **101**, 1418–1429.

### **Supporting Information**

Web Tables 1-6 and Web Figures 1-4 referenced in this article are available with this paper at the Biometrics website on Wiley Online Library. Software illustration of the proposed method is provided with this paper and also will be available online at Github.



(a) The average activity counts across all participants, along with the actual activity counts and survival time for five randomly selected participants by SEQN (unique subject identifier)



(b) The average of the first four L-moments of the time-varying physical activity profiles across all participants, as well as the first four L-moments for five randomly selected participants by SEQN, using log-transformation

**Figure 1:** Visual summary of physical activity across participants

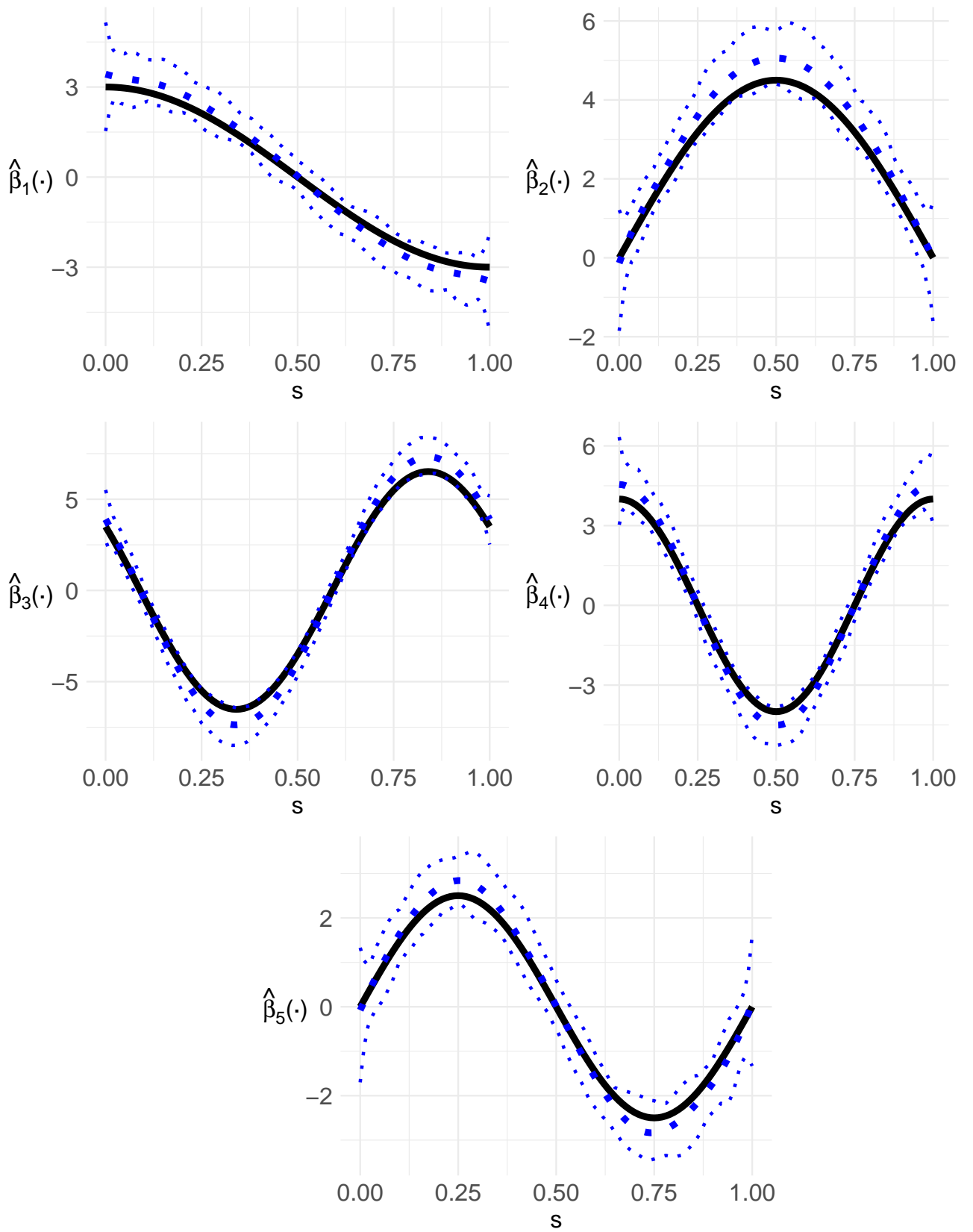


**Figure 2:** MC estimates and pointwise confidence intervals of the coefficient functions ( $n = 400$ ); ( $\cdots$ , VSF-COX; —, true curve)

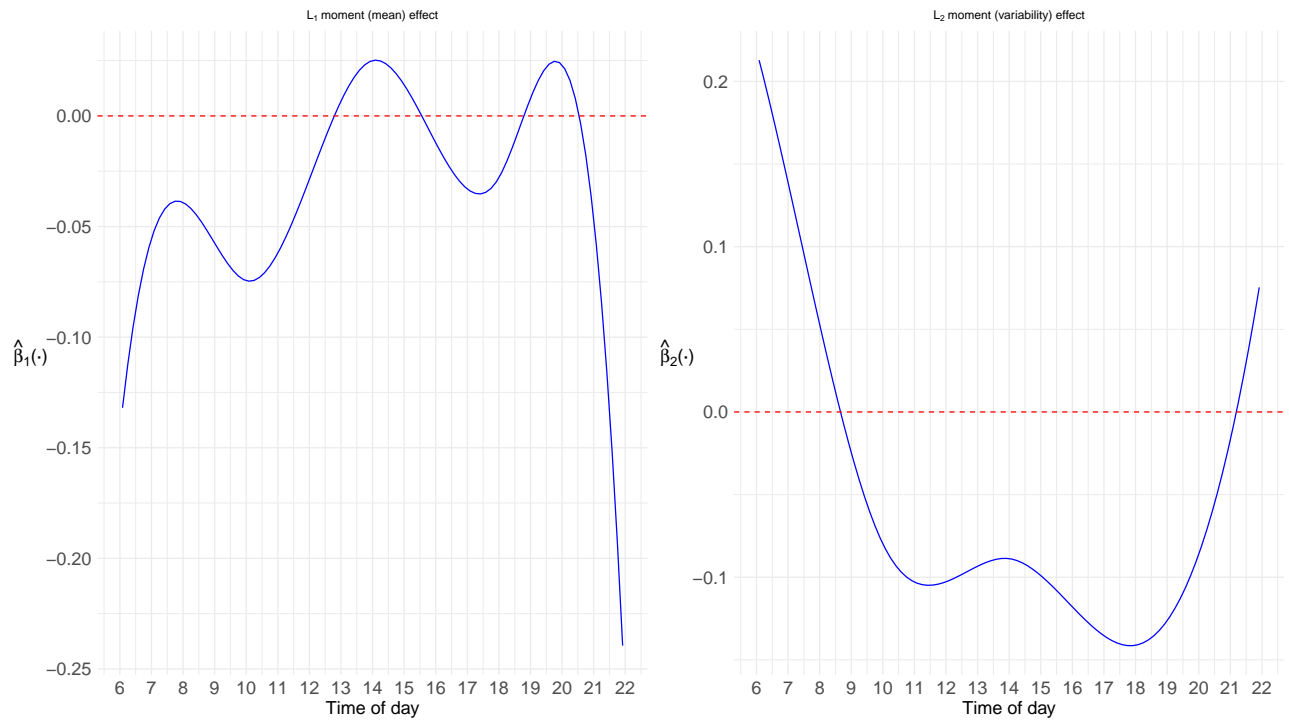


**Figure 3:** Estimated functional effects of the first ( $L_1$ ) and second ( $L_2$ ) moments over time from 6 a.m. to 10 p.m.

Table 1: Comparison of selection performance and average model size across different sample sizes

Sample size	Method	Variables	TPR	FPR	Average model size
200	grpregLASSO	scalar	0.993	0.920	32.965
		functional	0.993	0.932	
		all	0.993	0.927	
	VSFCOX	scalar	0.990	0.033	8.355
		functional	0.999	0	
		all	0.996	0.014	
400	grpregLASSO	scalar	1	0.265	13.95
		functional	1	0.185	
		all	1	0.220	
	VSFCOX	scalar	1	0.003	8.030
		functional	1	0	
		all	1	0.001	
800	grpregLASSO	scalar	1	0.308	15.235
		functional	1	0.236	
		all	1	0.268	
	VSFCOX	scalar	1	0	8.005
		functional	1	0	
		all	1	0	

Table 2: Comparison of MISE across different sample sizes

Sample size	$\hat{\beta}_1(\cdot)$	$\hat{\beta}_2(\cdot)$	$\hat{\beta}_3(\cdot)$	$\hat{\beta}_4(\cdot)$	$\hat{\beta}_5(\cdot)$
200	1.168	1.994	3.569	1.614	0.984
400	0.221	0.321	0.543	0.289	0.179
800	0.067	0.085	0.136	0.084	0.055



## Supporting Information for Variable Selection in Functional Linear Cox Model

Yuanzhen Yue<sup>1</sup>, Stella Self<sup>1</sup>, Yichao Wu<sup>2</sup>, Jiajia Zhang<sup>1</sup>, and Rahul Ghosal<sup>1,\*</sup>

<sup>1</sup>Department of Epidemiology and Biostatistics, University of South Carolina.

<sup>2</sup>Department of Mathematics, Statistics, and Computer Science, University of Illinois at Chicago.

\**email*: rghosal@mailbox.sc.edu

## 1. Web Appendix A

---

### Algorithm 1 Group descent algorithm for the VSFCOX method

---

Initialize  $\boldsymbol{\beta}^{(0)}, \boldsymbol{\gamma}^{(0)}$

**repeat**

  Compute linear predictor:  $\boldsymbol{\eta} \leftarrow \mathbf{Z}\boldsymbol{\beta} + \sum_{k=1}^K \tilde{\mathbf{Z}}_k^T \boldsymbol{\gamma}_k$

  Compute working residual:  $\tilde{\mathbf{r}} \leftarrow \boldsymbol{\Delta} - \mathbf{e}$

**for**  $j = 1, 2, \dots, p$

$$z_j \leftarrow \mathbf{Z}_j^T \tilde{\mathbf{r}} + \beta_j$$

$$\beta'_j \leftarrow F(|z_j|, \lambda, \phi) \frac{z_j}{|z_j|}$$

▷ Firm-thresholding

$$\tilde{\mathbf{r}}' \leftarrow \tilde{\mathbf{r}} - \mathbf{Z}_j(\beta'_j - \beta_j)$$

**for**  $k = 1, 2, \dots, K$

$$\mathbf{z}_k \leftarrow \tilde{\mathbf{Z}}_k^T \tilde{\mathbf{r}} + \boldsymbol{\gamma}_k$$

$$\boldsymbol{\gamma}'_k \leftarrow F(\|\mathbf{z}_k\|, \lambda, \phi)$$

$$\tilde{\mathbf{r}}' \leftarrow \tilde{\mathbf{r}} - \tilde{\mathbf{Z}}_k(\boldsymbol{\gamma}'_k - \boldsymbol{\gamma}_k)$$

**until** convergence

---

Expected event:

$$e_i = \sum_{j:i \in R_j} \delta_j \frac{e^{\eta_i}}{\sum_{k \in R_j} e^{\eta_k}}.$$

Firm-thresholding:

$$F(z, \lambda, \phi) = \begin{cases} \frac{S(z, \lambda)}{1 - 1/\phi} & \text{if } |z| \leq \lambda\phi \\ z & \text{if } |z| > \lambda\phi \end{cases}.$$

Soft-thresholding:

$$S(z, \lambda) = \begin{cases} z - \lambda & \text{if } z > \lambda \\ 0 & \text{if } |z| \leq \lambda \\ z + \lambda & \text{if } z < -\lambda \end{cases}.$$

**2. Web Tables**

[Table 1 about here.]

[Table 2 about here.]

[Table 3 about here.]

[Table 4 about here.]

[Table 5 about here.]

[Table 6 about here.]

**3. Web Figures**

[Figure 1 about here.]

[Figure 2 about here.]

[Figure 3 about here.]

[Figure 4 about here.]

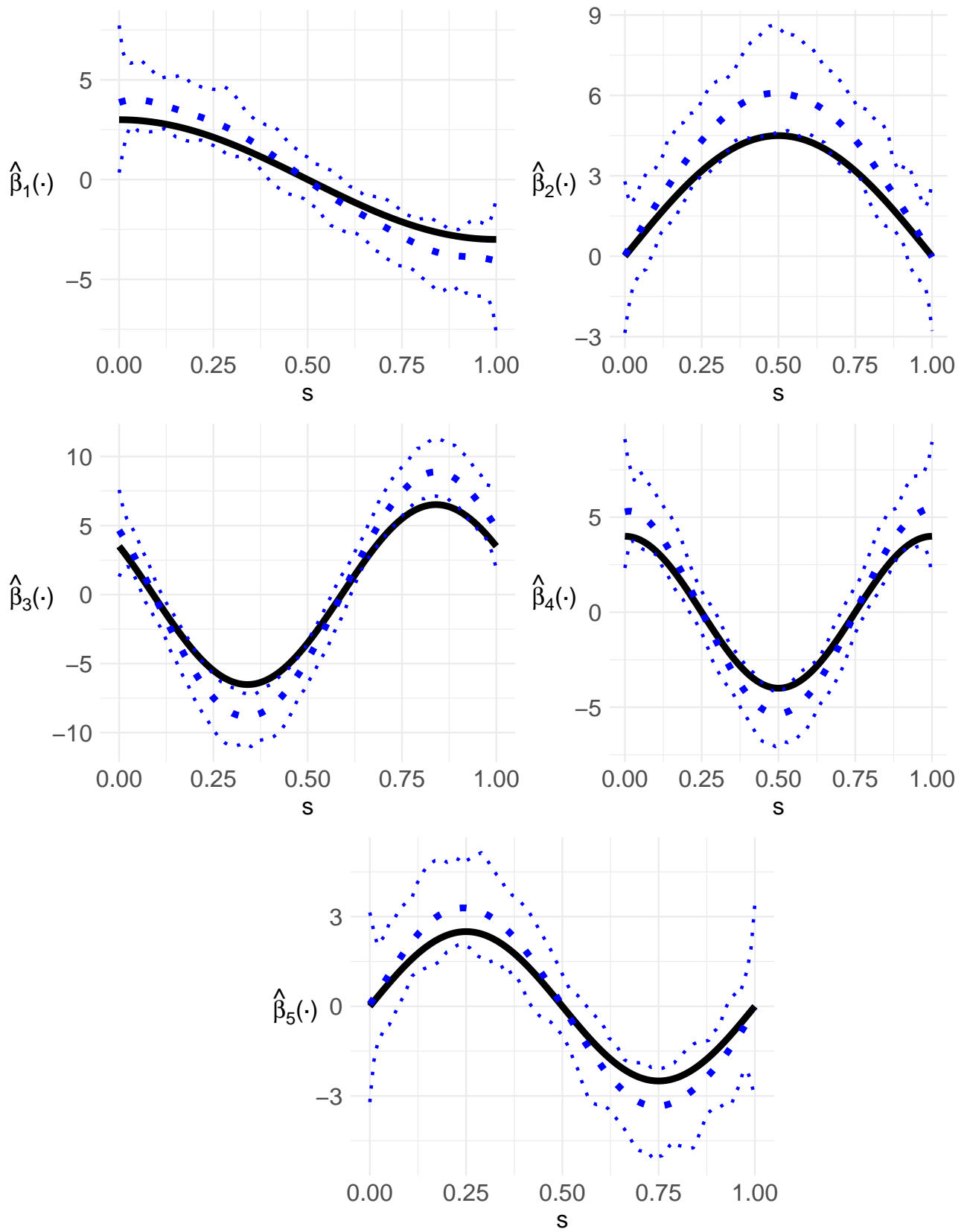


**Figure 1:** MC estimates and pointwise confidence intervals of the coefficient functions ( $n = 200$ ); ( $\cdots$ , VSF-COX; —, true curve)

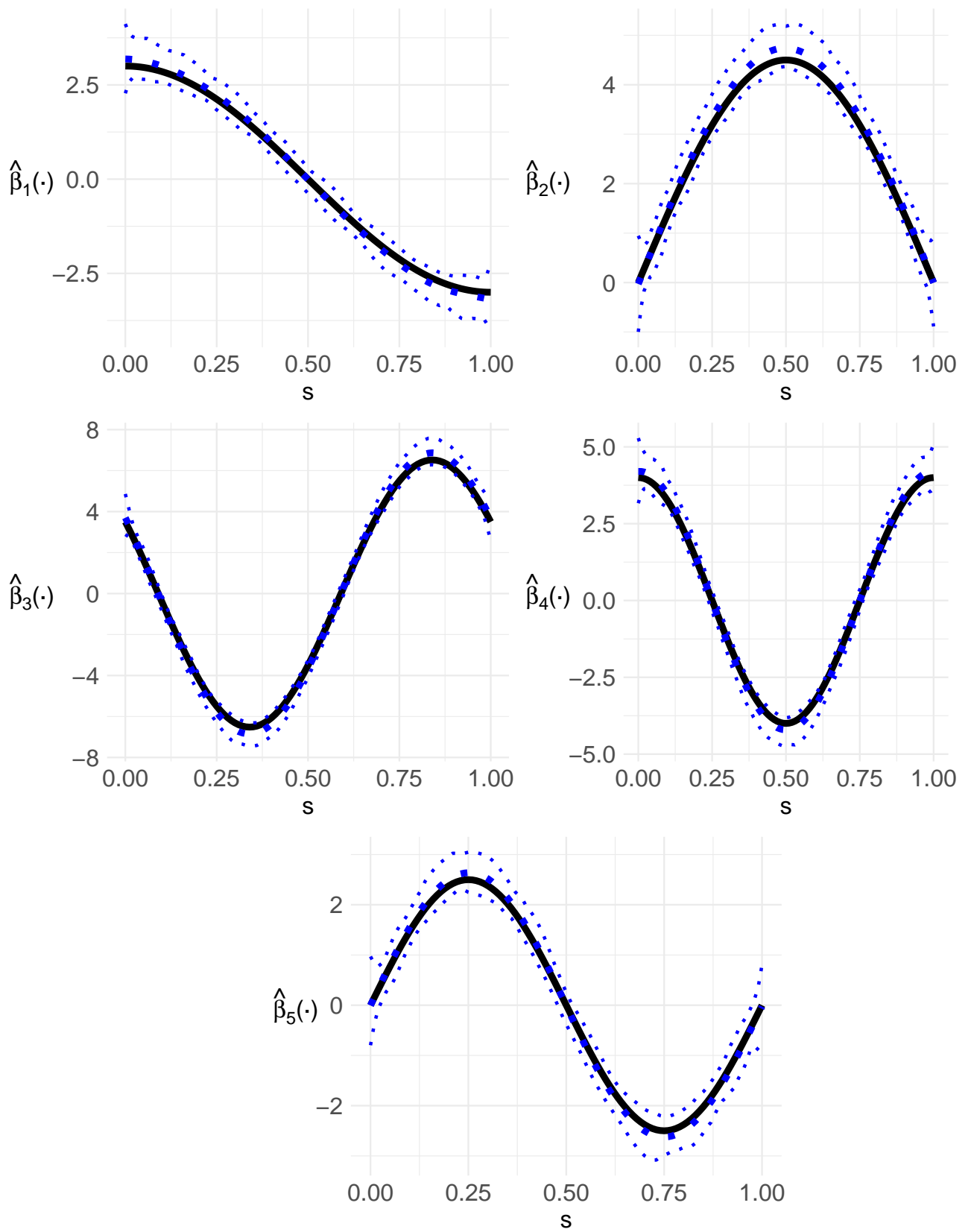


**Figure 2:** MC estimates and pointwise confidence intervals of the coefficient functions ( $n = 800$ ); ( $\cdots$ , VSF-COX; —, true curve)

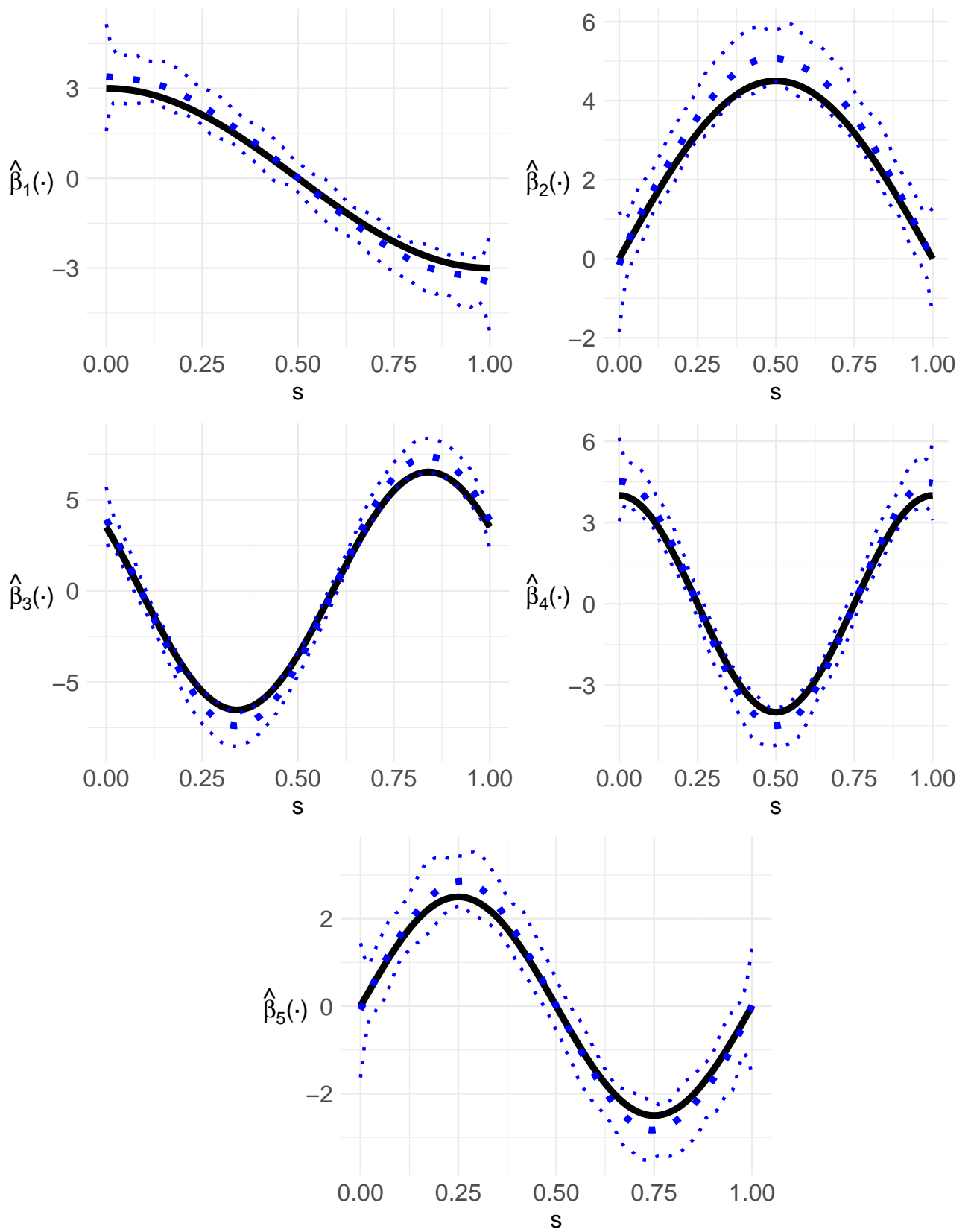


**Figure 3:** MC estimates and pointwise confidence intervals of the coefficient functions ( $n = 400$ ); ( $\cdots$ , VSF COX; —, true curve) - Adaptive Penalty

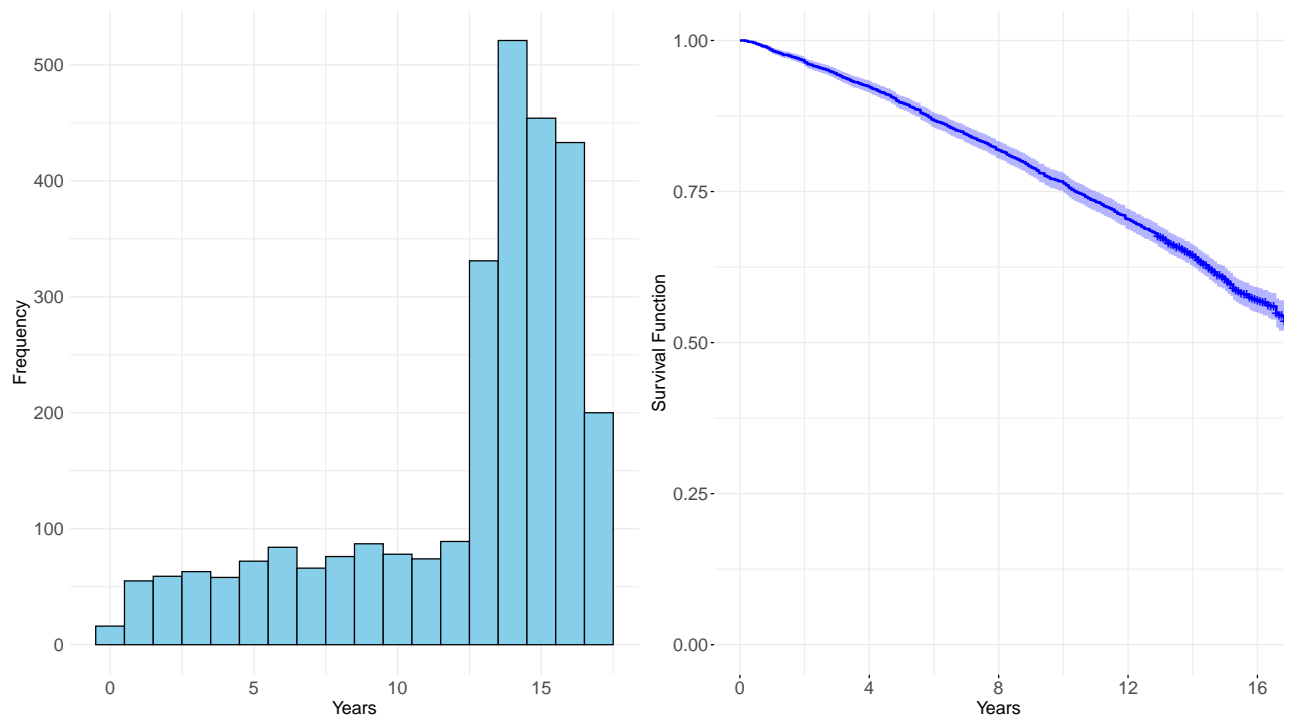


**Figure 4:** Histogram of survival time and Kaplan-Meier marginal survival curve

Table 1: Comparison of bias and MSE across different sample sizes

Sample size	$\hat{\beta}_1$		$\hat{\beta}_2$		$\hat{\beta}_3$	
	Bias	MSE	Bias	MSE	Bias	MSE
200	0.364	0.300	0.539	0.452	0.747	0.709
400	0.141	0.044	0.214	0.072	0.251	0.097
800	0.049	0.011	0.090	0.017	0.100	0.025

Table 2: Comparison of selection performance and average model size across different sample sizes - Adaptive Penalty

Sample size	Variables	TPR	FPR	Average model size
200	scalar	0.992	0.031	8.355
	functional	1.000	0.000	
	all	0.997	0.014	
400	scalar	1	0.003	8.035
	functional	1	0	
	all	1	0.001	
800	scalar	1	0	8
	functional	1	0	
	all	1	0	

Table 3: Comparison of bias and MSE across different sample sizes - Adaptive Penalty

Sample size	$\hat{\beta}_1$		$\hat{\beta}_2$		$\hat{\beta}_3$	
	Bias	MSE	Bias	MSE	Bias	MSE
200	0.345	0.268	0.553	0.447	0.778	0.768
400	0.138	0.041	0.208	0.069	0.251	0.095
800	0.051	0.011	0.087	0.017	0.105	0.025

Table 4: Comparison of MISE across different sample sizes - Adaptive Penalty

Sample size	$\hat{\beta}_1(\cdot)$	$\hat{\beta}_2(\cdot)$	$\hat{\beta}_3(\cdot)$	$\hat{\beta}_4(\cdot)$	$\hat{\beta}_5(\cdot)$
200	1.270	2.133	3.830	1.780	1.043
400	0.218	0.318	0.548	0.284	0.182
800	0.059	0.081	0.122	0.078	0.054

Table 5: Descriptive summaries of the scalar variables considered for the NHANES application

Characteristic	Mean (SD or Proportion)			p-value
	Overall (N = 2,816)	Survivor (N = 1,699)	Deceased (N = 1,117)	
Age	66.0 (9.6)	62.1 (8.0)	71.8 (8.9)	<0.001
Gender				<0.001
Male	1,431 (51%)	784 (46%)	647 (58%)	
Female	1,385 (49%)	915 (54%)	470 (42%)	
BMI	28.9 (6.0)	29.2 (6.0)	28.4 (5.9)	0.001
Smoking status				<0.001
Never	1,247 (44%)	848 (50%)	399 (36%)	
Former	1,097 (39%)	588 (35%)	509 (46%)	
Current	472 (17%)	263 (15%)	209 (19%)	

Table 6: Selected scalar variables and corresponding hazard ratios

	Age	Gender Female	Former Smoking	Current Smoking
Estimation	1.096	0.749	1.313	2.171